Dear reviewer and editor,

We want to start by thanking you for the positive general comments and good specific suggestions that we can use to improve the paper. We will address the comments below.

Questions from reviewer Henk Poulinder

This paper presents test results of new method to test if a wind turbine meets the grid codes using a voltage source converter. What I appreciate very much is that this paper does not report on more simulations (as many other publications do), but on a test setup that has been built to test wind turbines. Building a voltage source converter with a power level of 8 MW and controlling it with such dynamics that it can simulate grid faults is a huge engineering job. This setup makes it possible to do lots of other tests that the current test setups using voltage dividers cannot do.
The authors presented this idea in earlier publications. This paper presents test results that show the equipment works.

1. More than half of the paper presents test results: measurements of voltages, currents and powers under different circumstances. Can the test of fig 5 be omitted because it does not add anything to fig 6?

2. Doing a frequency scan is something that is possible with a VSC. However, why is that useful? What can we do with the results?
3 p9, line 1, I think the ramp is 12.5 pu/s instead of 0.0125 pu/s. Is that correct?

4. I miss a reference to what seems to be a similar paper: C Saniter; J Janning, "Test Bench for Grid Code Simulations for Multi-MW Wind Turbines, Design and Control", IEEE Transactions on Power Electronics, 2008, Volume: 23, Pages: 1707 - 1715.
What does the paper under review add to this one?

5. There are too many language mistakes. A number of examples:
p3 line 4: In every grid code it is specified => Every grid code specifies
p3 line 6: In fig. 1 is shown => Fig. 1 shows
p4 line 7: dependent of => dependent on
p4 line 24: can be of used to obtain => can be used to obtain
p7 line 10-13: unclear sentence
p9 line 14: as later see =>??
p12 line 3: signal of the wind turbine converter are => signals of the wind turbine converter are
p12 line 5: have being kept => have been kept
p12 line 7: dip => deep

Replay:

Dear Henk,

Thanks for the review, some comments follows, we have also updated the paper for most of your comments. Especially we have in a more clear way explained the benefits with frequency scan and improved the paper linguistically.

1. As explained in the text the LVRT control is not activated in the small dip test in fig 5 whereas in fig 6 the LVRT mode is activated and the control of active and reactive power starts a small oscillation in active and reactive power. And this can be a message for even larger transients

if the dip is lager. For this reason, we believe this case must stay in the paper. A note on this will be added to the paper.

2. This information is vital when, for example, analysing wind farm system data to identify the risk for sub-synchronous oscillations. This information is also valuable to evaluate the performance of large time-constant controller such as voltage control or power oscillations damping control that can be implemented in a wind turbine system or at wind farm level. A note on this will be added in the paper for better understudying of the reader.

3. Thank you for pointing this out. There is a m missing in pu/s,   pu/ms. It will be corrected in the next revision.

4. Thank you for the suggestion and for the interest in the topic. The abstract indicate that that paper describe the test setup and not the use of it in a real test with a large wind turbine A discussion will be added to our paper and the list of reference will be updated. In the new text can be read: "For example, the test setup presented in Saniter and Janning (2008) consists of a complex configuration of several VSCs and a three-winding transformer. The paper discusses a comparison between no-load tests and simulation results, while the effectiveness of actual tests remain"

5. Thank you for pointing this. The paper will be checked for proofread.

The editor also like us to explain the scientific value of the paper:

This paper has demonstrated that the full characterisation of the wind turbine system can be carried out by using flexible VSC-based test equipment. The full controllability of the test device allows for testing of multiple grid scenarios, making it possible not only to determine the behaviour of the generating unit against common grid contingencies, but also to evaluate the performance of the generating unit in further improving overall grid reliability. This includes evaluating different operating modes of the wind turbine which can be of interest for the overall stability of the interconnected power system.
The unique field tests presented in this report have provided an experimental validation of the proposed wind turbine testing methodology, particularly on the wind turbine impedance characterisation and on the evaluation of its steady-state and dynamic performance under different grid conditions.

To the knowledge of the authors a full scale tests with a 4 MW wind turbine have not been reported in the literature, especially where the generator and the converter performance are shown during the same test occasion.

In this paper we have highlighted the test methods for wind turbines by VSC and the theory, methods development with simulations are omitted in this paper. The theory part are referred to in the background chapter and are well described in the PhD-thesis of the first author Nicolas Espinosa.

Best regards

Ola Carlson and Nicolas Espinosa

Field-Test of Wind Turbine by Voltage Source Converter

Nicolás Espinoza and Ola Carlson

Department of Electrical Engineering, Chalmers University of Technology, Gothenburg, SE - 412 96, Sweden

Correspondence to: Ola Carlson (ola.carlson@chalmers.se)

Abstract. One of the main ~~challenge for the~~ challenges for wind energy development is ~~to make the~~ making wind turbines efficient in ~~respect of costswhile maintaining a~~ terms of costs, whilst maintaining safe and reliable operation. An important design criterion is to fulfil the grid codes given by the ~~fulfilment of Grid Codes given by~~ transmission system operators (TSO). ~~The Grid Codes~~ Grid codes state how wind ~~turbines/farms must behave~~ farms must perform when connected to the grid ~~in~~ under normal and abnormal conditions. In this regard, it is ~~well known~~ well-known that not all ~~the~~ technical requirements can be tested by using ~~the~~ actual impedance-based ~~testing equipment. For this reason, a testing equipment which comprises the use of~~ test equipment. Therefore, test equipment comprising a fully-rated Voltage Source Converter (VSC) in back-to-back configuration is proposed. Thanks to the full controllability of the applied voltage in terms of magnitude, phase and frequency, the use of VSC-based ~~testing equipment ,~~ test equipment provides more flexibility ~~as~~ when compared with actual ~~testing~~ test systems. As demonstrated in this paper, the investigated ~~testing device~~ test device not only can recreate any type of fault, including its recovery ramp~~and it~~ , but also can carry out steady-state tests, such as frequency ~~scan on the tested~~ variations and frequency scan, on the test object. Finally, test results ~~of a 4~~ from a 4.1 MW wind turbine and ~~an~~ 8 MW test equipment ~~,~~ located in Gothenburg, Sweden, are shown ~~in order~~ to validate the investigated grid code ~~testing~~ test methodology.

1 Introduction

The reliability of the electrical grid depends on how well the generating units, including wind energy systems, are prepared to ~~support the grid~~ provide support in case of ~~abnormal condition~~grid contingencies. In this regard, ~~Transmission System Operators~~ transmission system operators (TSOs) have ~~included in their Grid Codes~~ specific technical requirements ~~for interconnection of~~ included in their grid codes for connecting wind power plants ~~with~~ into the electricity grid. In general ~~words, a Grid Code~~ terms, a grid code specifies how a generating plant should behave ~~during~~ under normal and abnormal ~~condition of the grid~~ grid conditions. The continuous increase ~~of~~ in electrical energy from wind power injected into the power system has ~~lead~~ led TSOs to impose ~~more and more stringent requirements for this kind~~ ever more stringent requirements on these kinds of plants. ~~For this reason, it is~~ It is therefore crucial to develop ~~testing~~ test methodologies for this type of technology ~~in order to ensure a~~ to ensure correct integration of wind energy into ~~the~~ electricity grids (Espinoza, 2016).

To evaluate the capability of ~~the wind turbine~~ wind turbines to withstand grid disturbances, ~~today tests are performed~~ tests are currently carried out on the generating unit by using an impedance-based voltage dip generator (Yang et al., 2012). By developing further new ~~testing~~ test methodologies, it will be possible to test for grid scenarios other than voltage dips, ensuring

~~a~~ reliable and fault-tolerant operation of the wind turbine system. Furthermore, in the future, wind turbines will be required to participate more actively in ~~the regulation of the~~ regulating the grid (Tsiliand and Papathanassiou, 2009). In this regard, it is ~~well known~~ well-known that voltage source converters (VSC) can provide the necessary flexibility ~~in order~~ to control the terminal voltage as desired. On the other hand, ~~power~~ electronic devices have become cheaper and more accessible over the years (Blaabjerg and Ma, 2013). It is ~~, therefore ,~~ therefore natural that future ~~testing~~ test devices will be ~~fully, or if not, partially~~ partly or fully driven by VSC devices. For these reasons, a test run ~~has been carried out during~~ was carried out from January 2015 to August 2017 on ~~Big Glenn wind turbine (4~~ a 4.1 MW full-power converter (FPC) wind turbine ~~) by means of a full rated VSC-based testing equipment (~~(so called “Big Glenn” wind turbine) using a fully-rated 8 MW ~~VSC-HVDC)~~VSC-based test equipment.

2 Review of ~~Grid Code~~ grid code technical requirements

The ~~Grid Codes~~ grid codes considered in this section refer to countries ~~that have high penetration~~ with high levels of wind power penetration into their national ~~grid~~ grids (EWEA, 2016). Consequently, these countries have developed detailed technical requirements for grid interconnection of wind power plants (Espinoza et al., 2013).

The requirements for steady-state operation of the grid can be mainly ~~categorized in~~ categorised into three groups: reactive power requirements for normal voltage operation range; reactive power requirements during nominal active power production; and minimum operation time and active power curtailment during long-term frequency deviations.

These requirements have been compared in Tsiliand and Papathanassiou (2009), Espinoza et al. (2013), Mohseni and Islam (2012) and Altın et al. (2010). A dedicated analysis of the German ~~Grid Code~~ grid code is given in Erlich and Bachmann (2005). A specific analysis of the German grid code is given in Erlich and Bachmann (2005). Finally, control strategies developed ~~for meeting Grid Code~~ to meet grid code technical requirements have been documented in Bongiorno and Thiringer (2013), Molina et al. (2007) and Martinez and Navarro (2008).

2.1 Requirements for steady-state condition of the grid

A TSO can require reactive power injection from ~~the~~ wind farms to support overall system voltage control during normal ~~operation of the grid~~ grid operation. Usually, reactive power requirements are delimited ~~inside~~ within a minimum power factor range ~~that goes~~ from 0.95 lagging to 0.925 leading~~and for~~ , an active power set-point of between 0.05 pu and 1 pu ~~;~~ and within a nominal voltage ~~that varies~~ varying between 0.9 pu and ~~1.15~~ 1.1 pu.

Reactive power ~~requirement~~ requirements are also dependent on the active power production of the wind farm. For instance, the Danish ~~Grid Code (ENERGINETDK, 2010) states~~ grid code (ENERGINETDK, 2010) stipulates dependencies between voltage and reactive power ~~,~~ and between active and reactive power production. Both requirements ~~shall be complied~~ must be complied with simultaneously during normal ~~operation of the wind farm~~ wind farm operation. Moreover, reactive power injection can be controlled~~by either using~~ , with either a voltage control or power factor control (Tsiliand and Papathanassiou,

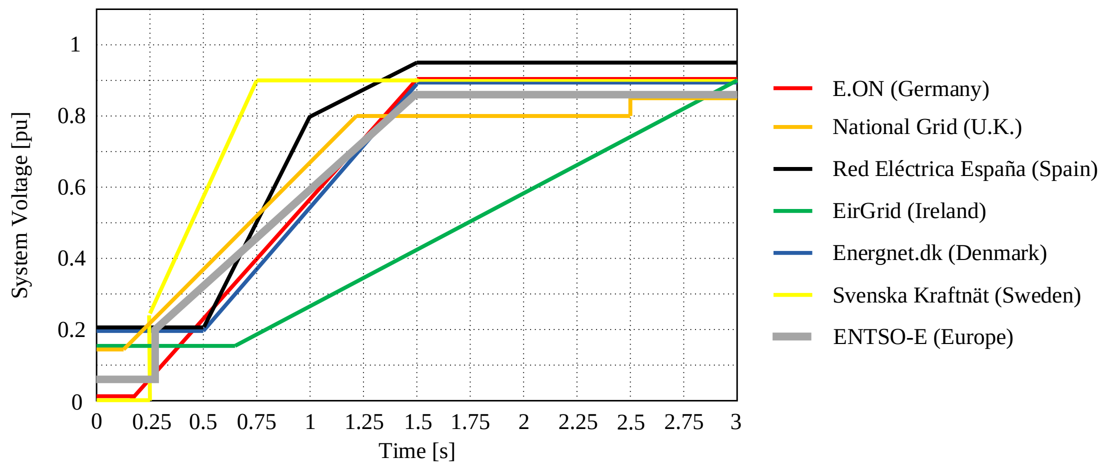

Figure 1. Example of LVRT profiles from the selected ~~Grid Codes~~grid codes.

2009). An ~~extra option to define the~~ additional option for defining reactive power production is to manually set the reactive power operating point if, for example, a continuous voltage deviation is present at the connection point~~is present~~. ~~In addition, in Grid Codes it is specified~~ Moreover, grid codes specify the steady-state frequency and voltage operation range ~~in~~ within which the wind turbine should operate continuously. ~~Normal~~ For voltages, normal condition is considered ~~for voltages close to~~ to be at 1.0 pu~~and frequency around~~ , with frequency of 50 ~~/~~or 60 Hz~~, with a~~ . A deviation of approximately ±0.1 pu from the rated voltage and ±0.5 Hz from the rated frequency ~~. Any steady-state~~ is also considered as normal condition. Any steady state grid condition outside these ~~values~~ boundaries is defined by a minimum operational time~~, and in~~ . In some cases, ~~by~~ a control action on the active power set-point of the wind farm ~~, as enforced by~~ can be requested by the TSOs, e.g.: the Danish (ENERGINETDK, 2010), Irish (EirGrid, 2015) and German (E.ON, 2006, 2008)~~TSOs~~. When active power curtailment is ~~demanded by the TSO~~ requested in case of frequency deviations, the generation unit must vary its active power output in order to contribute to the overall regulation of the system frequency. In ~~a severe case scenario~~ severe cases where the system frequency is outside the frequency operation band, the generating plant is allowed to disconnect.

2.2 Requirements for dynamic condition of the grid

Every ~~Grid Code~~ grid code specifies a voltage dip profile that the wind turbine should ride through without tripping. ~~An~~ An exhaustive comparison of LVRT profiles is given in Tsiliand and Papathanassiou (2009)~~. Low voltage ride through profilescharacterization~~ , while LVRT profiles, characterised in terms of fault time, retained voltage and recovery ramp rates can be found in Mohseni and Islam (2012). Figure 1 shows a combination of the strictest LVRT profiles among the selected ~~Grid Codes~~grid codes. In particular, the European ~~Grid Code ENTSO-E~~ grid code (ENTSO-E, 2016) defines the guidelines to establish the LVRT profiles in each network inside ~~EU~~European Union (EU).

When ~~it is~~ specified in the ~~Grid Code~~grid code, wind parks are required to support voltage restoration by injecting reactive power into the grid. ~~In particular~~Specifically, the generating plant must provide voltage support by injecting a specific amount of reactive current ~~during a voltage dip~~depending of the retained voltage at the connection point. For example, the Danish ~~Grid Code~~ grid code (ENERGINETDK, 2010) enforces a specific LVRT with a retained voltage of 0.2 pu per 500 ms, as shown in Fig. 1, and ~~demands for~~ stipulates reactive power support during voltage restoration. Reactive current must be injected ~~when~~ in a linear fashion when the voltage deviates below 0.9 pu. When the system voltage is lower than 0.5 pu, nominal reactive current ~~injection~~ must be reached.

2.3 Testing for ~~Grid Code~~ grid code fulfilment

The IEC 61400-21 standard issued by the International Electrotechnical Commission (IEC) defines the methodology ~~to test~~ for testing part of the ~~requirement stated in Grid Codes for interconnection of~~ technical requirement stipulated in grid codes, particularly for interconnecting wind turbines (IEC 61400-21 ed2.0, 2008). Moreover, ~~in order~~ specialised test equipment has been developed to fulfil the standard criteria ~~, specialized testing equipment has been developed~~ (Yang et al., 2012).

The most common ~~testing~~ test device for LVRT ~~test~~ testing of wind turbines is the impedance-based voltage dip generator (Beeckmann et al., 2010; Martinez and Navarro, 2008; Ausin et al., 2008) . The impedances ~~that constitute the testing~~ which constitute the test device are arranged ~~in order~~ to form a voltage divider at the terminals of the ~~tested object . By a proper selection of these~~ object being tested. By selecting the proper impedances, the amplitude and phase angle of the applied voltage can be controlled as desired. Although it has a simple and robust design which makes it modular and easily transportable, one of the main drawbacks of this ~~testing device is the fact that it is only able to apply voltage steps~~ test device is that can only be applied to voltage step variations due to the closing-opening action of the circuit breaker. Moreover, the device is highly dependent on the short-circuit power at the grid connection point, which will also impact the resulting wind turbine voltage (Ausin et al., 2008; Yang et al., 2012; Hu et al., 2009). Other devices have been developed in which the applicable voltage is controlled by VSC. For example~~testing~~ , the test setup presented in Saniter and Janning (2008) ~~consist of a highly-complex~~ consists of a complex configuration of several VSCs and a three-winding transformer~~while the paper discuss~~ . The paper discusses a comparison between no-load ~~test~~ tests and simulation results, while the effectiveness of actual tests remain undisclosed.

A simple and flexible solution to ~~realize~~ realise a voltage dip generator is to use two fully-rated VSCs in back-to-back configuration. By controlling the turbine-side output of the converter system, the effect of all ~~kind~~ kinds of grid faults can be emulated (Wessels et al., 2010). Thanks to the full controllability of the applied voltage in terms of magnitude, phase and frequency, the use of VSC-based ~~testing~~ test equipment, shown in Fig. 2, provides more flexibility ~~as compared with~~ compared to the standard impedance-based test equipment (Espinoza et al., 2013; Ausin et al., 2008)~~, and~~ . It also brings more advantages in terms of size and weight (Yang et al., 2012; Diaz and Cardenas, 2013). ~~In addition~~Furthermore, the AC grid is decoupled from the ~~tested object when performing the test; meaning thatthe strength of the grid is not a major limitation~~test object when conducting the test. This means that, if a proper control strategy ~~of~~ is implemented for the grid-side VSC of the test equipment~~is implemented~~, grid strength is not a major limitation.

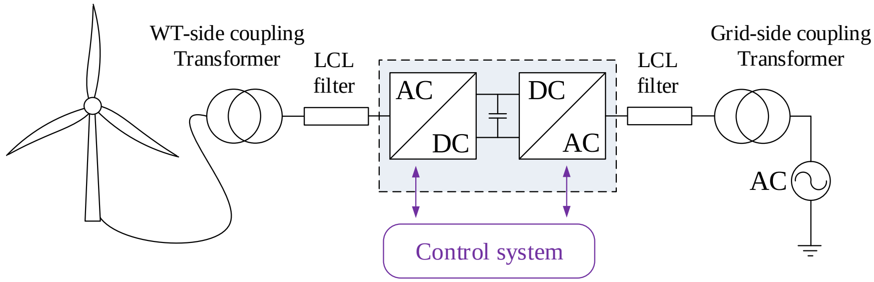

Figure 2. ~~Single line~~ Single-line diagram of a VSC-based test equipment.

Moreover, the LVRT profile given in the majority of the ~~Grid Codes~~ grid codes can be fully tested, including the recovery ramp (Espinoza et al., 2013), ~~allowing for the emulation of any kind of grid scenario applied to the tested object. Its~~ Such precise control allows ~~for more possibilities of tests that can be carried out besides what is normally required in the Grid Codes~~more test types to be conducted than normally required by grid codes. For example, frequency ~~characterization of wind turbines can be performed~~ support capabilities of the test object can be evaluated by conducting a test in which the fundamental frequency applied at the PCC is varied. On the other hand, a frequency characterisation of the wind turbine can be conducted by introducing asynchronous frequency content into the applied voltage while observing the equivalence admittance at the ~~Point of Common Coupling~~ point of common coupling (PCC)~~. Additionally, frequency support capabilities of the tested object can be evaluated by performing a test where the frequency applied at the PCC is varied, as later demonstrated .~~, as demonstrated later in this paper.

Since wind turbine data is not always available, the ~~testing~~ test equipment can be used to obtain more information from an actual wind turbine system (Espinoza, 2016). By using ~~a~~ fully controllable VSC-based ~~testing~~ test equipment, it is possible to determine how well the wind turbine ~~is able to~~ can reject frequency components other than the fundamental frequency. ~~In this regard~~Thus, the generating unit can be scanned ~~in~~ across a wider frequency range in which the wind turbine ~~can~~ could interact with other ~~existing elements~~ elements already present in the ~~interconnected grid.~~ interconnecting grid.

In this regard, frequency scan tests have been carried out ~~by means of the testing device to characterize~~ using the test device to characterise the input admittance of the ~~tested~~ wind turbine unit ~~. Here~~being tested. In this paper, this analysis is limited to the sub-synchronous range~~only~~. The implementation of the controller ~~on the testing equipment is also~~ in the test equipment is discussed in Espinoza (2016).

The main drawback of this technology is ~~the fact that~~ that it is more expensive than ~~using the standard testing~~ the standard test device introduced in the previous section. In addition, the control algorithm needed to implement such arrangement of VSC is more complex~~and~~ , while extra attention must be ~~given~~ paid when dealing with over-currents due to the use of sensitive power electronics. Moreover, to emulate a grid fault as realistically as possible, ~~a high dynamic performance of the controller that~~ the controller which computes the output voltage of the VSC ~~is necessary~~ needs to be of high dynamic performance (Lohde and Fuchs, 2009).

Figure 3. ~~Testing facility in~~ Gothenburg test facility, comprising the 4.1 MW FPC ~~“~~ÔÇ£Big Glenn~~”~~ ÔÇØ wind turbine~~; housing of~~ . The facility houses the back-to-back HVDC station ~~,~~ and coupling inductor (back) and AC filters (front)~~inside the house~~.

3 Description of the ~~testing~~ test facility

3.1 System layout

The ~~testing~~ test equipment is an 8 MW back-to-back HVDC station ~~placed in the harbour of~~ located at the harbour in Gothenburg, Sweden ~~. A picture of the actual wind turbine is given in Fig. 3 (Göteborg Energi AB). The~~ (Göteborg Energi AB). Figure 3 pictures the wind turbine itself. The turbine is located at the edge of the land ~~in proximity~~ and close to the sea. ~~During the majority~~ Most of the time, the wind turbine receives offshore wind from the northern part of Denmark. The station~~also shown in Fig. 3~~ , shown in the upper right corner of Fig. 3, houses the interconnecting ~~filters shown in Fig. 3~~ equipment shown at the bottom ~~right side. Moreover, a~~ of the figure. A diagram of the ~~layout of the wind turbine~~ wind turbine layout connected to the VSC-based ~~testing deviceis shown in Fig. 2, including~~ test device, including the VSC, interconnecting filters and coupling transformer~~which are located in the HVDC station~~, is shown in Fig. 2.

3.2 Description of the VSC-based test system

3.3 ~~VSC-based testing system description~~

The test equipment is rated ~~in~~ at 8 MVA at 10.5 kV. The wind turbine is coupled to the ~~testing~~ test device at the primary of the coupling transformer, as shown in Fig. 2. The secondary of the transformer is rated at 9.35 kV and its impedance 0.08 pu. An ~~*LCL*~~ LCL filter bank is placed ~~in order~~ to remove the harmonic content produced by the ~~turbine-side VSC~~ VSC itself. This converter controls the AC voltage imposed ~~to~~ on the wind turbine system, while the grid-side converter ~~is controlling~~ controls the DC-link voltage by exchanging active power with the interconnecting grid. The ~~testing~~ test equipment is interfaced with the ~~grid means of *LCL*~~ 10.5 kV grid using again an LCL filter bank and coupling transformer~~, which grid-side is again 10.5 kV. Note that the AC grid is decoupled from the tested object when performing the test; meaning that the strength of the grid is not a major limitation. Finally, between~~ . Finally, the wind turbine and ~~the testing equipment are interconnected~~ test equipment are connected by a 300 m cable.

In this installation, only the three-phase voltages and three-phase currents at the PCC are sampled by a computer located in the ~~control room of the HVDC station~~ HVDC station control room. The instantaneous active and reactive power are calculated off-line.

3.2.1 Control of the grid-side VSC

The main blocks ~~that constitute~~ comprising the implemented discrete controller are the DC voltage control~~and the inner current controller together with the~~ , inner current control and pulse-width modulator (PWM) block in cascade configuration and synchronized with the AC grid by means of a phase-locked loop (PLL). The ~~structure of a typical cascaded controller can be found in Espinoza (2016). The~~ outer DC voltage control generates the reference current for the ~~inner-current controllerof the grid-connected converter~~inner current controller. The output of the current controller is the reference voltage ~~value for the output voltage~~ at the terminals of the grid-side VSC. The output reference voltage is sent to a ~~pulse-width modulator (PWM)~~ PWM block which computes the gating ~~signals transistors of the VSC (Espinoza, 2016).~~ signal for the VSC transistors. The complete structure of a typical controller for this type of application can be found in Espinoza (2016).

3.2.2 Control of the turbine-side VSC

~~In~~ A dedicated open-loop voltage control is incorporated in the control algorithm of the turbine-side VSC of the test equipment~~, a dedicated open-loop voltage control is implemented~~. The output of the controller is the reference value for the ~~output voltage of the VSC~~ VSC terminal voltage. Finally, a PWM modulator is used to compute the switching signals of the converter (Espinoza, 2016).

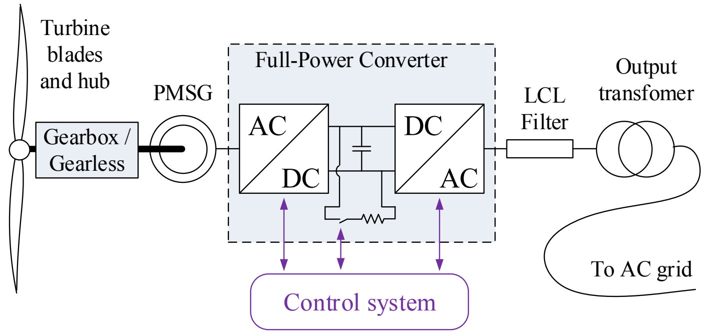

Figure 4. Schematic representation of an FPC wind turbine.

3.3 Big Glenn wind turbine

In an FPC wind turbine, the generator is connected to the grid through a full-power rated back-to-back VSC, as ~~depicted~~ shown in Fig. 4. ~~This configuration allows for an increased fault-tolerant capability of the wind turbine, avoiding severe transients in the generator when a grid fault occurs. Moreover, the grid-side converter of an FPC wind turbine can be designed and controlled in order to provide additional reactive power support, without having the need of over-magnetizing the generator core. Moreover, a~~ A gearbox is typically used to step-up the rotational speed when coupling the wind turbine hub with the generator shaft. In a direct-drive configuration similar to ~~the configuration~~ that found in Big Glenn ~~, i.e.: absence of the~~ (no gearbox in the drive train~~allowing a~~, allowing direct connection between ~~the hub and the rotor~~hub and rotor), a dedicated low-speed multi-pole generator must be used ~~in order~~ to achieve the desired nominal frequency in the stator terminals. The back-to-back VSC is then used to transfer the generated power to the AC grid, while allowing enough decoupling thanks to the DC-link between the two VSCs in Fig. 4. This configuration allows for an increased fault-tolerant capability of the wind turbine, avoiding severe transients in the generator when a grid fault occurs. Moreover, the grid-side converter of an FPC wind turbine can be designed and controlled to provide an additional reactive power support.

The use of fully-rated back-to-back VSC for grid interconnection of wind turbine generators allows ~~for~~ a fast response during abnormal ~~condition of the grid~~ grid condition (Beeckmann et al., 2010; Abram Perdana, 2014). For instance, during a voltage dip, ~~the~~ generated power cannot be delivered into the grid due to ~~the absence of sufficient~~ insufficient grid voltage. In this scenario, the grid-side-converter can quickly control the current output, avoiding feeding ~~fault currents of large magnitude~~ large-magnitude fault currents into the grid. The DC-link capacitor is protected by a DC-crowbar~~, which allows for the~~. This allows redirection of the produced power into a resistor~~providing a fast protection during DC over-voltages.~~, providing fast DC over-voltage protection.

The wind turbine under test is rated ~~in~~ at 4.1 MVA at 10.5 kV. The stator of the generator, having a voltage rating of 0.69 kV, is directly connected to the back-to-back VSC. The generator-side VSC, here operated in torque control mode, injects the generated power into the wind turbine DC-link capacitor. The grid-side VSC controls the DC-link voltage by exchanging active

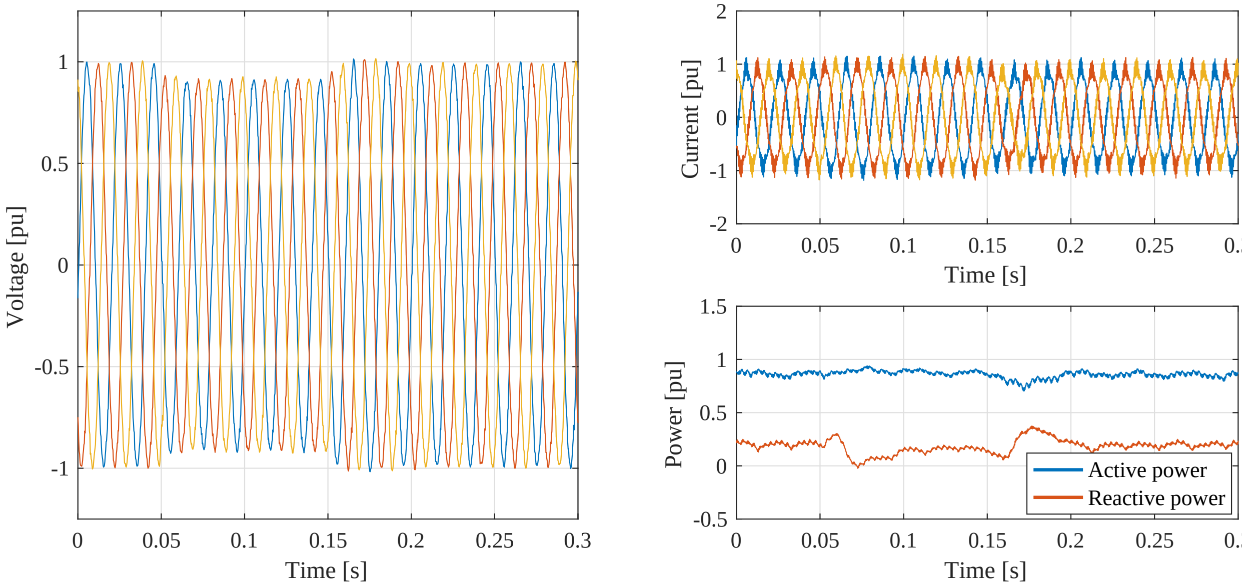

Figure 5. Wind turbine tested for voltage dip at full power production. ~~In~~ The figure ~~:~~ shows three-phase voltage and current, ~~and~~ plus active and reactive power output.

power with the imposed AC grid. A filtering stage is placed between the VSC and the LV-side of the wind turbine transformer in order to reduce the harmonic content injected into the electricity grid.

Finally, the output transformer of the wind turbine, with an impedance of 0.06 pu, steps-up the voltage from 0.69 kV to 10.5 kV. Information about wind turbine control during faults can be found in Espinoza (2016), Abram Perdana (2014), Espinoza et al. (2015).

4 Tests results

4.1 Testing for ~~Low Voltage Ride Through (~~LVRT~~)~~

One of the first tests carried out on the ~~testing facility corresponds~~ test facility on January 13th, 2015, corresponded to a voltage dip at full power production. The ~~following tests were conducted on January 13th, 2015. The~~ first attempt was to select a relatively small voltage variation, with a smooth transition between normal operation level and retained level. In order to ~~safely~~ conduct the experiment safely while learning the dynamics of the system, the voltage ~~is~~ was reduced from 1 pu to 0.9 pu for 100 ms. The results are shown in Fig. 5. In the following and in all plots, a base voltage of 10.5 kV and base power of 4.1 MVA is ~~utilized~~used.

The three-phase PCC voltage is shown in Fig. 5. At 0.05 s the voltage is reduced from 1 pu to 0.9 pu. At 0.15 s the voltage is brought back to 1 pu~~with a ramp function~~. In this test, a stiff ramp rate of 0.2 pu/ms has been selected for the inception of the voltage dip, while a ramp of 0.01 pu/ms has been set for the recovery. In order ~~for the wind turbine~~ to maintain constant

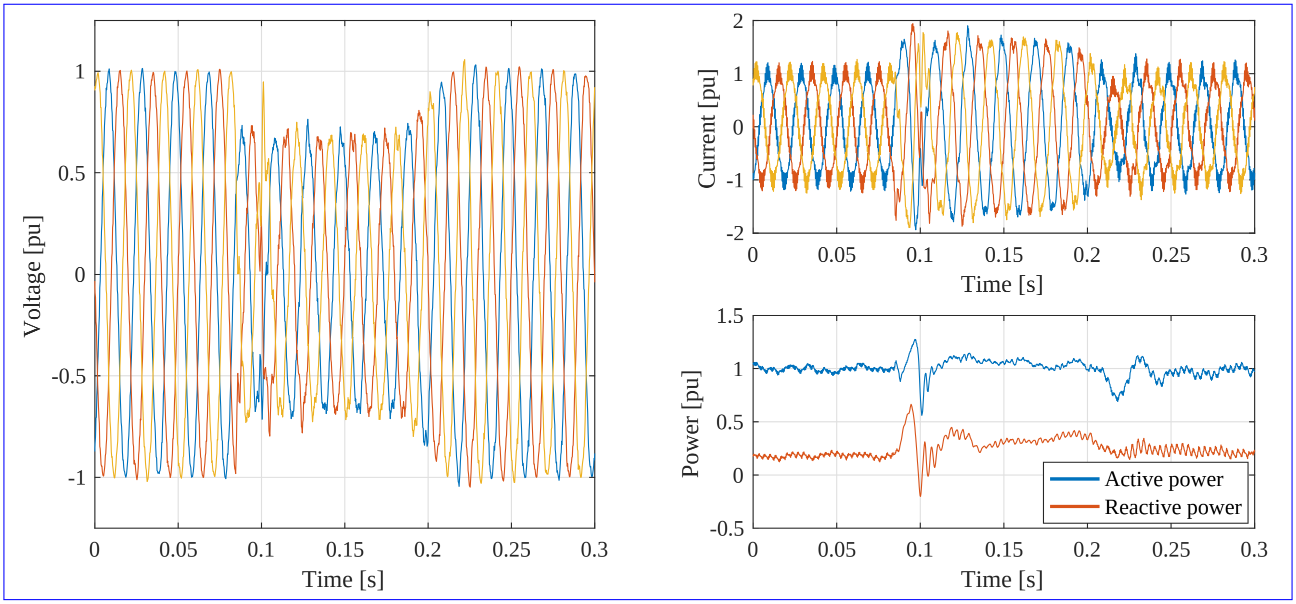

Figure 6. Wind turbine tested for LVRT at full power. figure shows three-phase voltage and current, plus active and reactive power output.

power production during the voltage reduction, the generating unit increases the magnitude of the current, while maintaining a constant power production, as also depicted in Fig. 5. During the voltage variation, the wind turbine maintains its active power set-point, injecting a steady 0.9 pu of active power into the imposed grid. From the figure, it ~~is possible to observe~~ can be observed that the wind turbine does not engage its LVRT control. Thus, the reactive power is ~~reduced only~~ only reduced due to the reduction of the voltage across the AC-link between the wind turbine and ~~the testing~~ test equipment.

A second test ~~has been~~ was carried out the same day and during the time in in which the wind turbine was still producing nominal active power. Here, the voltage ~~is~~ was varied from 1 pu to 0.65 pu for 100 ms ~~while the wind turbine is producing nominal active power. As compared with the test presented in Fig. 5~~with the same ramp-rates as previously mentioned. In this test, the LVRT control strategy of the wind turbine ~~is here activated . The results are depicted in presented Fig. 6. Moreover, the latter figure shows an indication on how sensitive fault-ride trough threshold~~ was activated during the voltage dip, providing an indication of how sensitive fault ride-through thresholds are set in the ~~tested object.~~ test object. The results are presented in Fig. 6.

The three-phase PCC voltage is dropped at ~~t=~~ 0.05 s. ~~In this test, a stiff ramp rate of 0.2 pu/ms has been selected for the voltage dip while a ramp of 0.01 pu/ms has been set for the recovery.~~ At 0.075 s, it is possible to observe a transient in both the current and ~~the~~ voltage shown in the figure. The transient lasts for 10 ms ~~and~~ while the wind turbine manages to control its current output during the voltage dip.

~~Wind turbine tested for LVRT at full power. In figure: three-phase voltage and current, and active and reactive power output.~~

The wind turbine active power set-point is maintained at 1 pu, while the reactive power is ~~boosted~~ 0.2 pu at pre-fault, reaching a mean value of 0.4 pu during the voltage dip. ~~Finally, it is possible to observe that the pre-fault reactive power exchange at the~~

~~measurement point is 0.2 pu. The wind turbine injects an additional 0.2 pu of reactive power when detecting the voltage dip at its terminals. Therefore, a total of 0.4 pu is maintained until the voltage is increased back to 1 pu.~~

~~The voltage starts to recover~~ The voltage starts its recovery at 0.18 s ~~with a~~ as per the ramp function. ~~Observe~~ Note that the current is also reduced at the same time ~~that~~ the reactive power is brought back to 0.2 pu. The active power oscillates at 0.23 s ~~while~~ when the voltage has reached a steady-state level of 1 pu. ~~Observe~~ Finally, observe that the current is above 1 pu during the voltage dip, meaning that the wind turbine have over-current capabilities and it is capable to momentarily increase the output current beyond nominal values during the ~~voltage dip~~contingency.

4.2 Reactive power control during voltage dip

A similar test ~~has been~~ was carried out on ~~the~~ 17th ~~of~~ May of 2016. Unfortunately, the wind turbine was operating at low wind speed. However, the lack of ~~produced active power~~ active power produced made the variations in ~~the~~ reactive power more prominent, as ~~later shown~~ shown later in this section. This experiment ~~consists in~~ consisted of a voltage variation from 1 pu to 0.75 for about 200 ms. ~~In order to~~ To avoid an oscillatory response similar to ~~the ones~~ those experienced in the previous experiment, the down-slope ramp of the controlled VSC voltage ~~is set at 0.02~~ was set at 0.04 pu/ms and ~~the recovery ramp is set at 0.006~~ recovery ramp at 0.0067 pu/ms. From the voltage waveform given in Fig. 7, it is possible to observe that the voltage is controlled by the ~~testing~~ test equipment in an effective and smooth way. Moreover, due to reduced ~~ramp-rate~~ slope at dip inception ~~, as compared to 10 times faster in Fig. 6,~~ the oscillatory response ~~is~~ shown in Fig. 6 was not triggered.

The active power was set to 0.15 pu during this test. ~~Moreover, the~~ The reactive power seen in Fig. 7 at pre-fault is mainly due to the capacitor bank of the local LCL filter placed at the terminals of the turbine-side VSC of the ~~testing~~ test equipment, while the variation observed during the voltage dip is due to the control action of the wind turbine.

~~When the~~ Note that the wind turbine injects reactive current when the voltage dip is detected at 0.12 s~~, the wind turbine injects reactive current~~. As shown in the figure~~above~~, the current ~~reaches 0.95~~ reached 1 pu, meaning that the turbine ~~is operated in proximity to the~~ was operated at rated current. ~~In order to~~ To quickly boost the voltage, the reactive power~~shown also in Fig. 7 is increased with~~ , also shown in Fig. 7, is increased using a ramp function. ~~There is a small overshoot in the current that is reflected on the reactive power at 0.14 s, mainly due to the fact that the voltage has reached steady-state during the dip while the current continues to increase. This can be attributed to the voltage monitoring system and the reactive power controller of the wind turbine during dynamic condition of the grid.~~

~~The reactive power~~ Reactive power injection is maintained for the complete duration of the voltage dip. The (mainly reactive) three-phase current is later reduced~~when~~ , once the voltage is restored to 1 pu. Note that the current is maintained ~~during a short period of time~~ briefly at 0.85 pu, while the voltage has already started to increase towards 1 pu. ~~The system reaches a post-fault steady-state at 0.43 s. It can be observed that there is a~~

A small transient on the reactive power set-point ~~after the voltage dip~~can be observed both at fault inception and recovery. This can be attributed to the ~~wind turbine~~ voltage monitoring system and the dynamics of the reactive power controller of the wind turbine; particularly, to the wind turbine control action when calculating a reactive current reference based ~~to a varying instantaneous~~ on a varying measured voltage. Afterwards, the wind turbine ~~will resume~~ resumes normal operation, reducing the

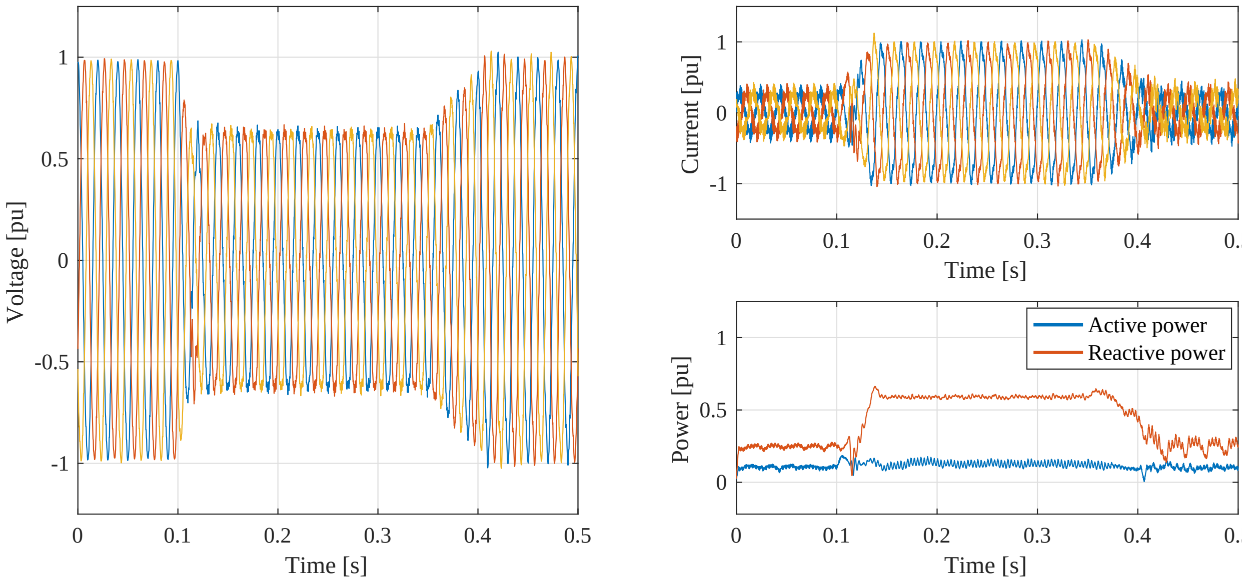

Figure 7. Wind turbine tested for LVRT at low power production. In figure: three-phase voltage and current, and active and reactive power output.

current (and therefore the reactive power output) to its pre-fault operating point. The system reaches a post-fault steady-state at 0.43 s.

4.3 Testing for unbalance voltage dip

~~In this section~~ This section studies the response of the wind turbine under unbalanced voltage dip~~is studied~~. This test was ~~carried out again on the~~ conducted on 17th ~~of~~ May of 2016, ~~at~~ under low wind conditions. ~~The~~ Here, the turbine-side VSC of the actual ~~testing~~ test equipment is controlled in an open-loop and the ~~voltage in phase a and b~~ voltages in phases a and b are dropped from 1 pu to 0.7 pu for 200 ms. The resulting PCC voltage is given in Fig. 8. During the duration of the test, the voltage in phase c is maintained at 1 pu from the VSC output. However, due the negative sequence across the AC circuit between ~~test-VSC~~ test device and wind turbine, phase c appears ~~to be slight~~ slightly lower than 1 pu at the measurement point. Moreover, observe from the power plot in Fig. 8 that the reactive power is increased from approximately 0.25 pu to 0.35 pu~~approximately, while a~~. A relatively small oscillation at 100 Hz in both active and reactive power is seen~~. The distorted current shown in Fig. 8 accounts for oscillations seen in the power, although these oscillations are small~~, mainly due to the small negative sequence present in the current.

These last three examples ~~show in a clear way~~ clearly illustrate the response of the wind turbine, particularly the reactive power controller during a balanced and unbalanced voltage dip. ~~Considering that the control system of the~~ Given that the tested wind turbineÔÇÖs control system is unknown, these results suggest that the controller ~~implemented on the wind turbine accounts also~~ may also account for the negative sequence, ~~while~~ whilst still experiencing small oscillations in its output power.

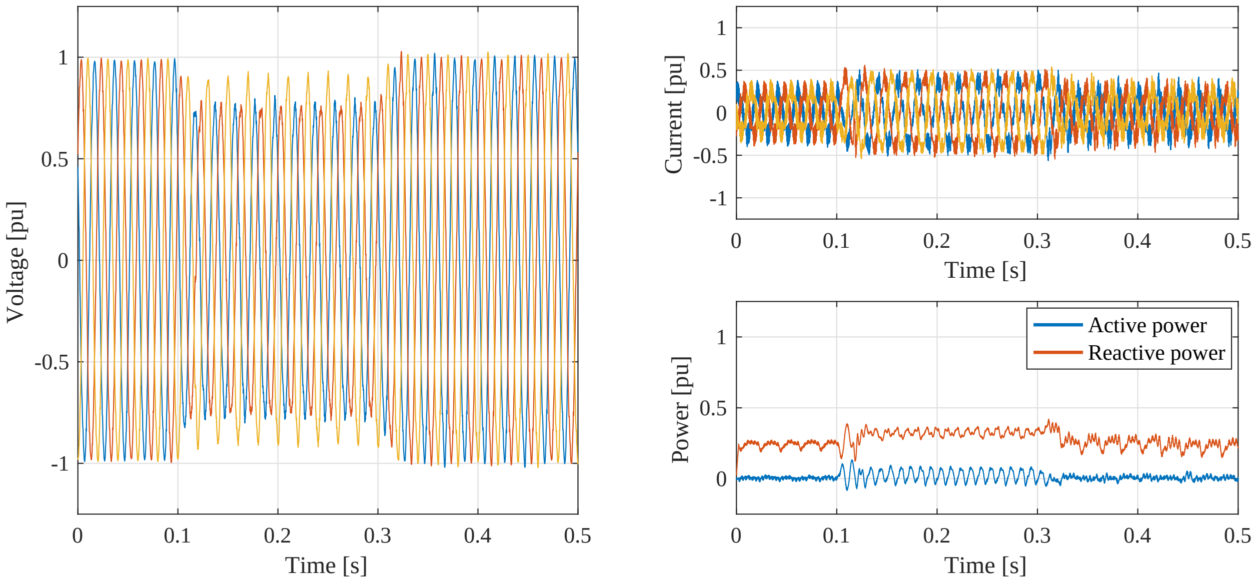

Figure 8. Wind turbine tested for unbalanced voltage dip at low power production. ~~In~~ figure ~~:~~ shows three-phase voltage~~and~~ , current and active and reactive power output.

4.4 Impact of the voltage dip in wind turbine converter

A voltage dip applied at the VSC terminals of the ~~VSC of the testing equipment affect drastically the voltage of the~~ test equipment drastically affects the wind turbine converter voltage. Moreover, the grid-side VSC controller of the wind turbine ~~VSC will also react against~~ will react to the voltage dip measured at the ~~LVÔÇôside~~ LV-side of its output transformer~~(where the local LCL filter is~~ , particularly at the grid-side LCL filter shown in Fig. 4~~)~~. Although the measured voltage will be somewhat smooth ~~because of the filtering action of the overall inductance~~due to the wind turbine transformer impedance and filtering stage, the resulting output current and DC voltage of the back-to-back ~~wind turbine converter~~ VSC are controlled in such way that the wind turbine can maintain normal operation ~~as~~ when possible. In ~~the following~~this regard, the internal signals of the wind turbine converter ~~is~~ are plotted for the case ~~given~~ in Fig. 6 and the effect of the voltage dip test is further discussed below. ~~. For a better understanding of the dynamics inside the wind turbine converter, the physical magnitudes of speed, voltage and power have been kept, while the measured torque and mechanical power at the generator are shown in percentage of their nominal values.~~

If the voltage reduction ~~is not dip enough~~does not dip sufficiently, the wind turbine might have some extra room in its rating ~~in order~~ to maintain normal power production at a reduced voltage (see Fig. 5). This can be done by increasing the current immediately after detecting a voltage dip. In ~~Fig. 9 it is possible to observe~~ this regard, Fig. 9 shows the effect of a voltage dip in the wind turbine converter. The voltage imposed is measured at 1 pu and is dropped to 0.74 pu for approximately 150

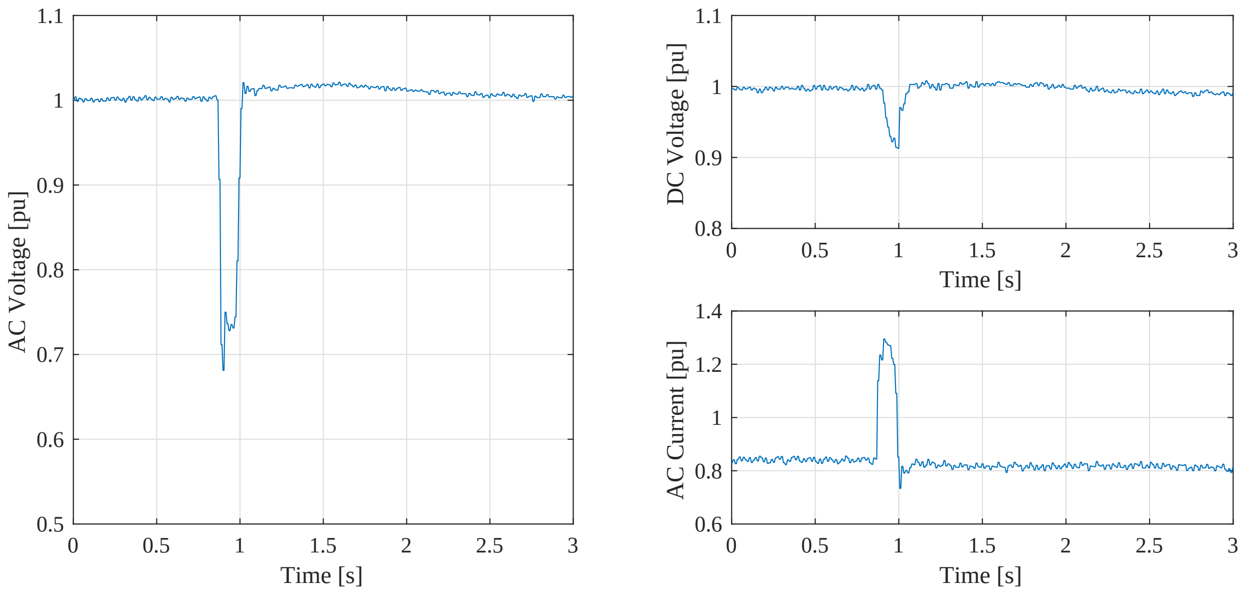

Figure 9. Wind turbine VSC under a ~~non-severe~~ voltage dip. ~~In~~ The figure ~~:~~ shows AC voltage resulting at the LV-side of the wind turbine transformer and DC voltage and AC current magnitude measured at the grid-side VSC.

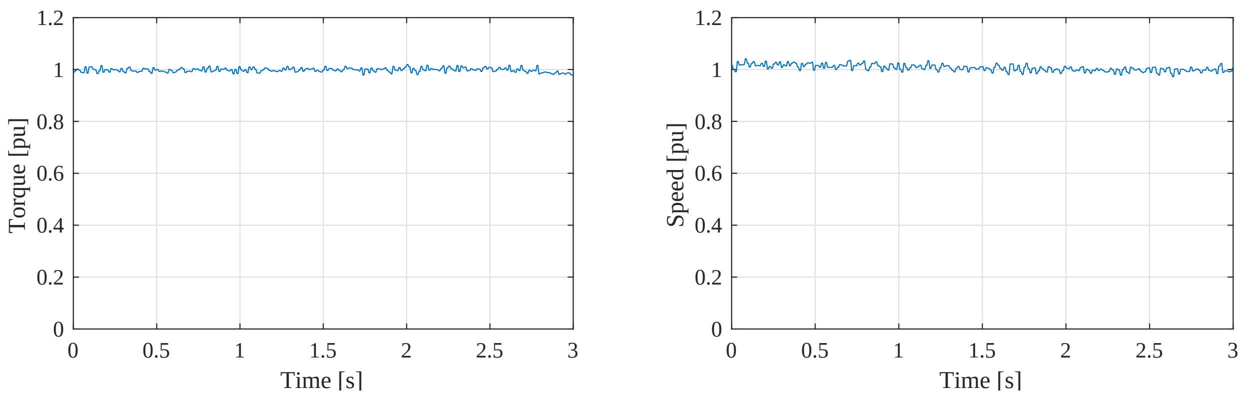

Figure 10. Wind turbine VSC under a ~~non-severe~~ voltage dip. ~~In~~ The figure ~~:~~ shows generator torque and ~~generator~~ speed.

ms~~approximately. The~~. The VSC line current is also plotted in Fig. 9 and ~~it increases fast~~ increases rapidly when the voltage dip is detected at 0.08 s. ~~The~~ Its pre-fault value is 0.85 pu and rises to 1.3 pu during the dip.

The DC voltage (also shown in Fig. 9) is dropped during the test. This can be attributed to the ~~fast increasing in the~~ rapid increase in wind turbine current, which can be faster than the time constant of the DC link ~~capacitor, allowing~~ capacitors at the wind turbine converter. This allows a normal power flow during the dip while ~~affecting slightly or even decreasing~~ slightly disturbing the DC voltage.

Finally, it is interesting to see the decoupling that ~~exist~~ exists between the grid-side VSC and the generator-side VSC of the wind turbine. Figure 10 shows the generator torque and ~~generator~~ speed when the grid voltage experiences a dip. If the conditions are met ~~so that~~ for the wind turbine VSC response ~~is~~ to be smooth, the generator is ~~not affected. Here~~unaffected. Here, the torque is maintained ~~constant at~~ at a constant 1 pu and the speed is also controlled at 1 pu~~as well, meaning that~~. This means the wind turbine system is operated at full power. Note that the wind turbine converter ~~have~~ has over-current capabilities ~~in order~~ to maintain a constant power flow during transients.

4.5 Testing for frequency deviation

In this case study, the voltage applied to the wind turbine is controlled at 1 pu and only the fundamental frequency is varied. The ~~obtained results are given~~ results are shown in Fig. 11. ~~In order to measure for a long period of time~~ To measure for long time period, voltage and current are ~~here measured by a portable measurement~~ measured using a portable unit installed at the turbine-side of the VSC-HVDC station~~shown in Fig. 3. Particularly, at the converter-side of the coupling transformer in ??~~. The unit is placed between the coupling transformer and the LCL filter shown in Fig. 3. For this reason, the reactive power curve ~~depicted~~ (shown in red in Fig. 11) has a different value ~~with respect~~ compared to the other case studies shown ~~throughout~~ in this paper.

~~Here~~In the following, only the measured frequency and ~~the~~ active and reactive power ~~output~~ outputs are shown. The first scenario corresponds to a frequency drop of 0.5 Hz for 15 seconds. From the first case shown in Fig. 11, it can be ~~noticed~~ observed that the frequency ~~is varied~~ varies with a ramp of 0.2 Hz/s, or 5 seconds per varied Hz, for both the drop and ~~the~~ recovery of the frequency. According to the Swedish ~~Grid Code~~ grid code (Svenska Kraftnät, 2005), the wind turbine should maintain its active power production at any given frequency within the specified normal frequency range~~(~~, i.e.: from 49.5 Hz to 50.5 Hz~~)~~; while varying its output power for frequencies outside this range and ultimately ~~cease~~ ceasing to operate at frequencies outside the full operational range~~(~~, i.e.: 48 Hz to 52 Hz~~)~~. The upper plot ~~in Fig. 11~~ for frequency dip in Fig. 11 shows that the active power is kept constant at 0.7 pu for ~~the majority of the~~ most of the time during the test. At 30 s, the active power is slightly reduced, mainly due to ~~the variations in the wind speed at the moment of the~~ variations in wind speed during the test.

The second scenario corresponds to two consecutive frequency swells of 1 Hz. The frequency is initially controlled at 50 Hz and varied upwards with a ramp of 0.05 Hz/s, or 20 seconds per varied Hz. A frequency of 51 Hz is maintained for approximately 25 seconds~~approximately. Afterwards, the frequency is~~. The frequency is then increased to 52 Hz. The results are shown ~~in the right-side~~ on the right-hand side of Fig. 11 .

Observe in the lower plot that the ~~upwards and downwards~~ upward and downward tendency of the output power ~~suggest~~ suggests that the wind turbine ~~is varying~~ varies its operating point according to ~~the~~ wind speed and not ~~in demand of~~ with demand for the applied frequency. In addition, the active power ~~is slightly increased~~ increases slightly 10 seconds after the frequency reaches 51 Hz, at 40 s, while ~~continues to increase with the increasing of the system frequency~~ continuing to increase as the system frequency increases, at 60 s. ~~Finally, a~~ A critical point is finally encountered at 80 s when the frequency reaches 52 Hz. The wind turbine enters ~~into an operation mode that~~ an operational mode which affects the active power output~~while~~ ,

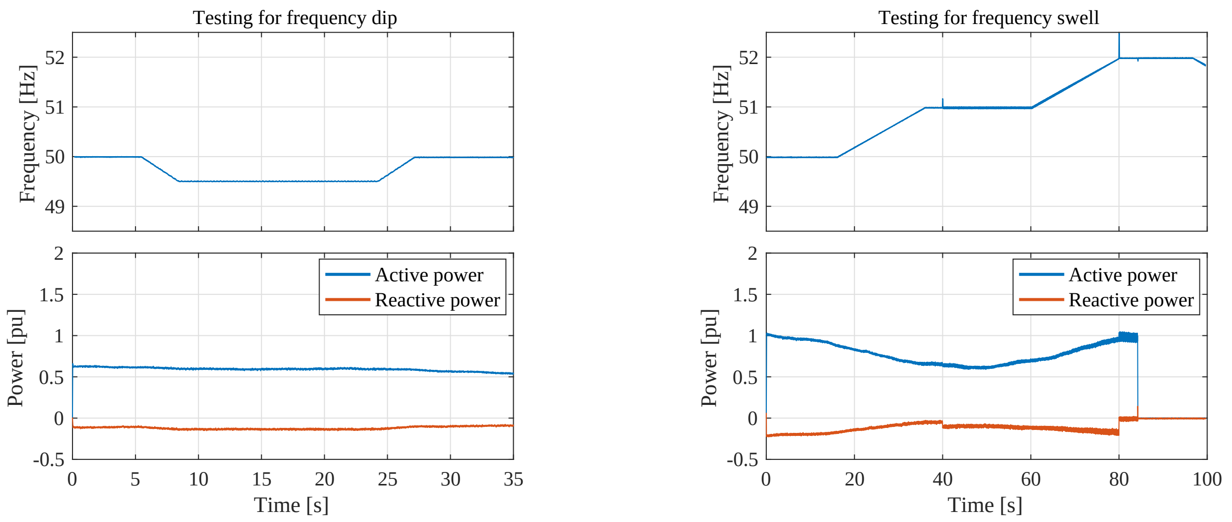

Figure 11. Frequency variation test~~. In figure: ~~, showing set-points of active and reactive power during frequency dip (left-side figures) and frequency swell (right-side figures).

whilst experiencing an oscillation at ~~104~~ roughly 100 Hz. The wind turbine shuts down~~by~~ , via an over-frequency protection relay, ~~5~~ five seconds after the frequency reaches 52 Hz, at t=85 s. The different power production levels experienced when ~~performing~~ conducting the test are also somewhat reflected ~~on~~ in the reactive power output of the wind turbine, as seen in the red traces for both scenarios ~~shown~~ in Fig. 11 .

4.6 Frequency scan

~~Carry on~~ Conducting a frequency scan on a wind turbine generator can provide valuable information about how the tested system behaves ~~in~~ across a wider frequency range. This information is vital when, for example, analysing wind farm system data to identify ~~e.g.: the risk for~~ issues such as the risk of sub-synchronous oscillations; ~~the risk for~~ risk of interaction with other elements ~~of the interconnecting grid such as~~ in the interconnecting e.g.: underwater cables or filter banks ~~in case of off-shore wind farms; as well as wind turbine~~ (for offshore wind farms), or interaction with active devices~~such as~~ , such as a Static Synchronous Condenser (STATCOM). ~~In addition, the~~ The investigated method can ~~provide information in order to evaluate the stability as well as the~~ also provide information for evaluating the stability and performance of large time-constant controllers, such as voltage control or power ~~oscillations damping control implemented~~ oscillation damping (POD) control installed in a wind ~~turbine systemor at wind farm level~~energy system.

~~First~~Firstly, this section shows the frequency scan test carried out on ~~the~~ 20th ~~of~~ June, 2016, when the wind turbine was operating at 0.6 pu power of production. Afterwards, the result ~~from~~ of the frequency scan test ~~,~~ carried out on ~~the~~ 17th ~~of~~ May, 2016, at low power production, is then given. The current and voltage are again measured at the HVDC station ~~, where~~ controlling the voltage applied to the wind turbine~~is controlled~~. The frequency scan is ~~performed~~ conducted by adding a voltage

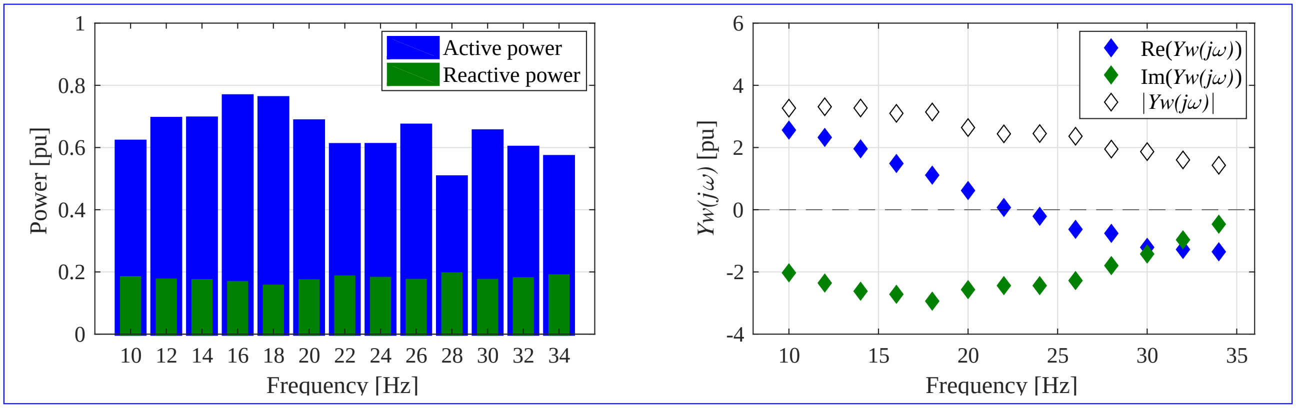

Figure 12. Results of frequency scan on the wind turbine operated at ~~56~~65% of power production. ~~In~~ The figure ~~:~~ shows operating points prior the scan ~~; measured~~ and admittance components measured.

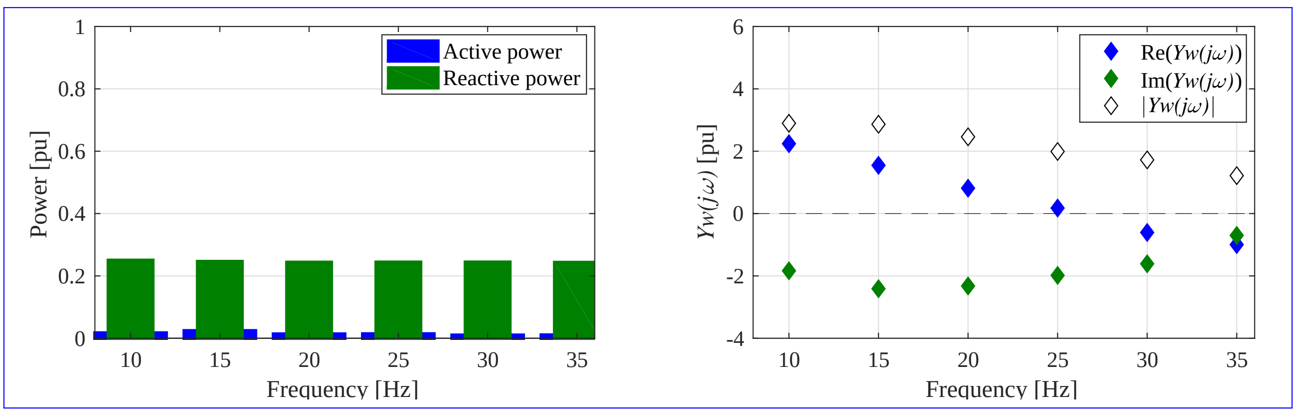

Figure 13. Results of frequency scan on ~~the~~ wind turbine operated at ~~65~~55% of power production. ~~In~~ The figure ~~:~~ shows the operating points prior the scan ~~; measured~~ and admittance components ~~.~~measured

component of magnitude 0.015 pu ~~modulated at the interested frequency , on top of~~ (modulated to the frequency being scanned) to the fundamental reference voltage of 1 pu. The measured phase voltage and line current are evaluated at the frequency of interest ~~by~~ and using the methodology given in Espinoza (2016), also reported in Espinoza et al. (2016).

~~The wind turbine is changing~~ During the scan, the wind turbine changed its operating conditions during each tested frequency~~and these are shown in Fig. 12 in bars~~. The average ~~output power~~ power output of the wind turbine is ~~of~~ measured at 2.9 MW. However, a wide variation between 2.6 MW and 3.5 MW ~~has been~~ was encountered during the test~~. The~~ , as shown in Fig. 12 as bars of different length. For each scan at a given frequency, the wind turbine impedance $Z_\mathrm{w}(j\omega)$ is obtained as an average of the phase impedances~~. The~~ , while each phase impedance is computed with the corresponding voltage and current vector measured at the frequency of interest and averaged within the sampling period.

The wind turbine admittance $Y_{\mathrm{w}}(j\omega)$ can be calculated by the inverse of $Z_{\mathrm{w}}(j\omega)$. The real and imaginary ~~part together with the~~ parts, plus magnitude of the measured phase admittance $Y_{\mathrm{w}}(j\omega)$ are shown in Fig. 12 ~~with~~ as blue and green dots respectively. The magnitude of the admittance is plotted ~~in~~ as white dots. The resulting measured points in Fig. 12 suggest that the wind turbine presents a positive real part for frequencies below 22 Hz, with a maximum measured value of 2.8 pu at 10 Hz. On the other hand, a relatively high non-passivity behaviour is ~~exhibit~~ seen for frequencies above 30 Hz, meaning that the wind turbine could resonate if these frequencies are encountered in the network. The minimum value for $Re(Y_{\mathrm{w}}(j\omega))$ is -1.5 pu and can be observed at the last scanned frequency of 34 Hz.

The scanned imaginary part of the admittance $Im(Y_{\mathrm{w}}(j\omega))$ is also shown in Fig. 12 ~~in~~ as green dots. The turbine seems to ~~present a~~ exhibit capacitive behaviour for most of the studied frequency range. ~~The~~ Note that the reactive power set-point at the measurement point is dependent on both the configuration of the filtering stage at the ~~terminals of the~~ VSC-HVDC terminals and on the wind turbineÔÇÖs reactive power controller. The minimum value of $Im(Y_{\mathrm{w}}(j\omega))$ is found to be -2.4 pu at 18 Hz, exhibiting its maximum capacitance in the scanned frequency range. For frequencies above 20 Hz, $Im(Y_{\mathrm{w}}(j\omega))$ increases ~~up~~ to a maximum of -0.4 pu measured at 34 Hz, corresponding to its minimum capacitance in the ~~synchronous~~ sub-synchronous range. Observe, however, that the reactive power set-point shown Fig. 12 is kept relatively constant at 0.2 pu (0.9 MVAr) at 50 Hz ~~during all~~ throughout the test.

The absolute value of the measured wind turbine admittance $|Y_{\mathrm{w}}(j\omega)|$is also shown in ~~in Fig. 12 in~~ Fig. 12 as white dots. ~~The~~ Note that the operating point of the wind turbine ~~at the moment of each test impacts both the amplitude and also the vector components of its input admittance~~during each scan impact not only the amplitude of the admittance but also its vector components. For this reason, the uneven trend of $|Y_{\mathrm{w}}(j\omega)|$ somewhat matches the variation on the output power of the wind turbine at each scanned frequency.

Finally, a second frequency scan is given in Fig. 13. The test was ~~carried out in a very low windy day ; therefore~~conducted on a day with very little wind; thus, the wind turbine ~~is operated~~ was operating at low power production. The figure shows the active and reactive power set-points at the moment of each test. Moreover, it ~~is possible to note~~ can be noted that the power flow ~~is mainly dominated~~ was dominated mainly by reactive power coming from the filter banks between ~~the~~ wind turbine and ~~the testing equipment . The~~ test equipment with a measured reactive power is ~~0.023 pu for all~~ 0.23 pu throughout the test. The calculated admittance ~~components are shown in dots also in Fig. 13~~ magnitude and its real and imaginary components are also shown in Fig. 13 as white, blue and green dots, respectively.

The real ~~part of the admittance~~ component $Re(Y_{\mathrm{w}}(j\omega))$ ~~, show in blue dots in Fig. 13, is slightly reduced to 2.2 pu, as compared to 2.8 pu given for the previous case. The~~ shows a reduction of 0.3 pu in its magnitude, if compared with the previous scan. However, the main difference is ~~the~~ its zero-crossing~~of the real part~~, which in this case occurs at 26 Hz, instead of 23 Hz for mid-power operation. From the plots where the reactive power is given, ~~this second tests~~ the second test shows a small increase in the reactive power measured at the HVDC station. Thus, ~~the imaginary part of the measured admittance~~ $Im(Y_{\mathrm{w}}(j\omega))$ can be affected by the operating point of the wind turbine, making the green trace in Fig. 13 slightly closer to 0 pu, as compared with Fig. 12. Finally, ~~the total magnitude~~ $|Y_{\mathrm{w}}(j\omega)|$ ~~of the admittance~~ is decreased from 4 pu ~~from~~ in the first test, to 2.7 pu when operated at no power~~, as shown in white dots in the figure~~. Observe that the trend of $|Y_\mathrm{w}(j\omega)|$ is somewhat smoother given that the wind ~~turbines operates a low power during the complete~~ turbine operates at low power for the full duration of the scan.

5 Conclusions

~~In this paper it has been~~ This paper has demonstrated that the full ~~characterization~~ characterisation of the wind turbine system can be carried out by ~~the use of a~~ using flexible VSC-based test equipment. The full controllability of the ~~testing~~ test device allows for testing of multiple grid scenarios, making it possible not only to determine the behaviour of the generating unit against common grid contingencies, but also to evaluate the performance of the generating unit in further improving ~~the overall reliability of the grid~~ overall grid reliability. This includes ~~, for example, the evaluation the operating modes that are of~~ evaluating different operating modes of the wind turbine which can be of interest for the overall stability of the interconnected power system.

Field test results ~~of~~ from the Big Glenn 4.1 MW wind turbine and 8 MW ~~testing~~ test equipment have been included in this paper. The tests carried out on the actual wind turbine system ~~include~~ included not only balance and unbalanced voltage dips, defined by different retained voltage and different ramp-rates, ~~as well as~~ but also frequency variation tests and frequency ~~scan~~scans. The results ~~shows~~ show that a LVRT control strategy is implemented ~~on~~ in the tested system ~~injecting~~ that injects reactive power when a voltage dip is detected. Moreover, it has been shown that the generating unit maintains ~~a~~ smooth control of the reactive power output even during unbalanced voltage dips, at least for low power set-points. These results demonstrate that a VSC-based ~~testing~~ test device can be used to evaluate how well a wind turbine system can withstand the technical requirements given in the ~~Grid Codes~~grid codes.

The multi-megawatt FPC wind turbine system has also been ~~characterized~~ characterised in the sub-synchronous range ~~by means of~~ using the interconnected VSC-based ~~testing~~ test equipment. The frequency scanning technique has been demonstrated by field test and the input admittance of the generating unit has been evaluated ~~for~~ under two operating conditions. The frequency trend of the scanned turbine exhibits a non-passive behaviour at higher frequencies within the sub-synchronous range, while also exhibiting capacitive behaviour throughout the ~~whole~~ complete scanned range.

The unique field tests presented in this report have provided an experimental validation of the proposed wind turbine testing methodology, particularly on the wind turbine impedance ~~characterization~~ characterisation and on the evaluation of its steady-state and dynamic performance ~~against different conditions of the grid~~ under different grid conditions.

Acknowledgements. ~~This work has been~~ This work was carried out within the Swedish Wind Power Technology Centre (SWPTC). The financial support provided by ~~the~~ academic and industrial partners including Göteborg Energi, Protrol, the Västra Götaland Region and the Swedish Energy Agency is gratefully acknowledged.

References

Altın, M., Göksu, O., Teodorescu, R., Rodriguez, P., Jensen, B. B., and Helle, L.: Overview of recent grid codes for wind power integration, in: Optimization of Electrical and Electronic Equipment (OPTIM), 2010 12th International Conference on, pp. 1152–1160, https://doi.org/10.1109/OPTIM.2010.5510521, 2010.

Ausin, J. C., Gevers, D. N., and Andresen, B.: Fault ride-through capability test unit for wind turbines, Wind Energy, 11, 3–12, https://doi.org/10.1002/we.255, http://dx.doi.org/10.1002/we.255, 2008.

Beeckmann, A., Diedrichs, V., and Wachtel, S.: Evaluation of Wind Energy Converter Behavior during Network Faults - Limitations of Low Voltage Ride Through Test and Interpretation of the Test Results, in: 9th International Workshop on Large-Scale Integration of Wind Power into Power Systems as well as on Transmission Networks for Offshore Wind Power Plants, 2010.

Blaabjerg, F. and Ma, K.: Future on Power Electronics for Wind Turbine Systems, Emerging and Selected Topics in Power Electronics, IEEE Journal of, 1, 139–152, https://doi.org/10.1109/JESTPE.2013.2275978, 2013.

Bongiorno, M. and Thiringer, T.: A Generic DFIG Model for Voltage Dip Ride-Through Analysis, Energy Conversion, IEEE Transactions on, 28, 76–85, https://doi.org/10.1109/TEC.2012.2222885, 2013.

Diaz, M. and Cardenas, R.: Matrix converter based Voltage Sag Generator to test LVRT capability in renewable energy systems, in: Ecological Vehicles and Renewable Energies (EVER), 2013 8th International Conference and Exhibition on, pp. 1–7, https://doi.org/10.1109/EVER.2013.6521629, 2013.

ENTSO-E: ENTSO-E Network Code for Requirements for Grid Connection Applicable to all Generators, https://www.entsoe.eu, 2016.

Erlich, I. and Bachmann, U.: Grid code requirements concerning connection and operation of wind turbines in Germany, in: Power Engineering Society General Meeting, 2005. IEEE, vol. 2, pp. 1253–1257, https://doi.org/10.1109/PES.2005.1489534, 2005.

Espinoza, N.: Wind Turbine Characterization by Voltage Source Converter Based Test Equipment, Doktorsavhandling PhD Thesis, Chalmers tekniska högskola. Ny serie, no: 4195, Department of Energy and Environment, Electric Power Engineering, Chalmers University of Technology, 2016.

Espinoza, N., Bongiorno, M., and Carlson, O.: Grid Code Testing of Full Power Converter Based Wind Turbine Using Back-to-Back Voltage Source Converter System, in: EWEA 2013 Annual Event Conference Proceedings, http://www.ewea.org/, 2013.

Espinoza, N., Bongiorno, M., and Carlson, O.: Novel LVRT Testing Method for Wind Turbines Using Flexible VSC Technology, Sustainable Energy, IEEE Transactions on, 6, 1140–1149, https://doi.org/10.1109/TSTE.2015.2427392, 2015.

Espinoza, N., Bongiorno, M., and Carlson, O.: Frequency characterization of type-IV wind turbine systems, in: 2016 IEEE Energy Conversion Congress and Exposition (ECCE), pp. 1–8, https://doi.org/10.1109/ECCE.2016.7855126, 2016.

Göteborg Energi AB: Göteborg Wind Lab, http://www.goteborgwindlab.se.

Hu, S., Li, J., and Xu, H.: Comparison of Voltage Sag Generators for Wind Power System, in: Power and Energy Engineering Conference, 2009. APPEEC 2009. Asia-Pacific, pp. 1–4, https://doi.org/10.1109/APPEEC.2009.4918228, 2009.

Lohde, R. and Fuchs, F.: Laboratory type PWM grid emulator for generating disturbed voltages for testing grid connected devices, in: Power Electronics and Applications, 2009. EPE '09. 13th European Conference on, pp. 1–9, 2009.

Martinez, I. and Navarro, D.: Gamesa DAC converter: the way for REE grid code certification, in: Power Electronics and Motion Control Conference, 2008. EPE-PEMC 2008. 13the, pp. 437–443, https://doi.org/10.1109/EPEPEMC.2008.4635305, 2008.

Mohseni, M. and Islam, S. M.: Review of international grid codes for wind power integration: Diversity, technology and a case for global standard, in: Renewable and Sustainable Energy Reviews, vol. 16, pp. 3876–3890, https://doi.org/http://dx.doi.org/10.1016/j.rser.2012.03.039, http://www.sciencedirect.com, 2012.

Molina, M., Suul, J. A., and Undeland, T.: A Simple Method for Analytical Evaluation of LVRT in Wind Energy for Induction Generators with STATCOM or SVC, in: Power Electronics and Applications, 2007 European Conference on, pp. 1–10, https://doi.org/10.1109/EPE.2007.4417780, 2007.

Saniter, C. and Janning, J.: Test Bench for Grid Code Simulations for Multi-MW Wind Turbines, Design and Control, IEEE Transactions on Power Electronics, 23, 1707–1715, https://doi.org/10.1109/TPEL.2008.925425, 2008.

Abram Perdana: Dynamic Models of Wind Turbines, Chalmers University of Technology, Gothenburg, Sweden, http://www.chalmers.se/, 2014.

EirGrid: EirGrid Grid Code Version 6.0, EirGrid, 2015.

ENERGINETDK: Technical regulation 3.2.5 for wind power plants with a power output greater than 11 kW, Energinet.dk, 2010.

E.ON: Grid Code - High and Extra High Voltage, E.ON Nets GmbH, Bayreuth, Germany, 2006.

E.ON: Requirements for Off-Shore Grid Connection in the E.On Nets Network, E.ON Nets GmbH, Bayreuth, Germany, 2008.

EWEA: Wind in Power, 2015 European statistics, The European Wind Energy Association, http://www.ewea.org/, 2016.

IEC 61400-21 ed2.0: Wind turbines - Part 21: Measurement and assessment of power quality characteristics of grid connected wind turbines, International Electrotechnical Commission, Germany, 2008.

Svenska Kraftnät: The Business Agency Svenska kraftnats regulations and general advice concerning the reliable design of production plants, Svenska Kraftnat, 2005.

Tsiliand, M. and Papathanassiou, S.: A review of grid code technical requirements for wind farms, in: IET Renewable Power Generation, vol. 3, pp. 308 – 332, https://doi.org/10.1049/iet-rpg.2008.0070, 2009.

Wessels, C., Lohde, R., and Fuchs, F.: Transformer based voltage sag generator to perform LVRT and HVRT tests in the laboratory, in: Power Electronics and Motion Control Conference (EPE/PEMC), 2010 14th International, pp. T11–8–T11–13, https://doi.org/10.1109/EPEPEMC.2010.5606830, 2010.

Yang, Y., Blaabjerg, F., and Zou, Z.: Benchmarking of Voltage Sag Generators, in: IECON 2012 - 38th Annual Conference on IEEE Industrial Electronics Society, pp. 943–948, https://doi.org/10.1109/IECON.2012.6389164, 2012.